AIChE

Fine Particle Turbulence Modulation

David Harbottle, Simon Biggs, and Michael Fairweather
Institute of Particle Science and Engineering, School of Process, Environmental and Materials Engineering, University of Leeds, Leeds LS2 9JT, U.K.

DOI 10.1002/aic.12388
Published online September 17, 2010 in Wiley Online Library (wileyonlinelibrary.com).

Streamwise turbulence intensities of fine particulate suspensions were studied in a 26 mm N.B. horizontal pipe loop. Colloidal silica spheres were prepared in 10^{-4}M and 1M KNO_3 solutions to control the degree of aggregate formation in the suspension. Using an ultrasonic Doppler velocity profiling sensor, the turbulence intensities of the fine particle suspensions were compared with those of a particle-free flow over a range of Reynolds numbers. At low electrolyte concentration, the silica particles remain dispersed, with the turbulence intensity of the suspension flow comparable with that of the particle-free flow. At high electrolyte concentration, increased particle-particle interaction leads to the formation of particle aggregates which support turbulence augmentation over a critical Reynolds number range. The range of Reynolds numbers over which this turbulence enhancement is observed is limited by both fluid dynamic effects at low Reynolds numbers ($\mathrm{Re} \approx 5500$*) and aggregate breakup at high Reynolds numbers (*$\mathrm{Re} \approx 8000$*).* © 2010 American Institute of Chemical Engineers *AIChE J*, 57: 1693–1699, 2011

Keywords: turbulence modulation, colloidal particles, aggregation

Introduction

Transportation of solid particles in a gas/liquid carrier phase is ubiquitous in the process industries. Such systems have been studied both experimentally and theoretically for many decades, particularly looking at transportation regimes,[1,2] deposition velocities,[3–7] and re-suspension characteristics.[8–11] In recent years, there has been significant interest in turbulence modulation,[12–15] where the presence of particles in a fluid has been observed to either enhance or dissipate the level of turbulence. Early reviews on turbulence modulation were published by Hetsroni[16] and Gore and Crowe.[14] Hetsroni[16] considered much of the published literature prior to 1989. The author discussed the conditions for turbulence modulation in terms of the particle relaxation time (t*) to characteristic eddy turnover time (t_e) ratio, and the particle Reynolds number. Gore and Crowe[14] compared data from several different authors so that the influence of flow geometry, flow Reynolds number, solids concentration and density ratio could be considered. Based solely on the particle diameter (d_p), the characteristic length scale of the most energetic turbulent eddies (l_e), and independent of the Re, the authors identified a demarcation ($d_p/l_e \approx 0.1$) between turbulence intensity augmentation and attenuation. For systems satisfying $d_p/l_e > 0.1$, the authors stated that the turbulence intensity augmentation is associated with the secondary flow turbulence in the wake behind a particle, while for systems satisfying $d_p/l_e < 0.1$ the turbulence attenuation is associated with the energy transfer from the turbulent eddies to a particle being translated in the flow. In the Gore and Crowe publication,[14] one significant data set was omitted from the turbulence intensity plot (Fig. 2 in the original publication). The study of Maeda et al.[17] was not included as a centerline turbulence intensity increase was measured for the gas transport of both 45 and 135 μm glass particles in a 56 mm pipe at $Re = 21{,}000$. With turbulence augmentation not satisfying $d_p/l_e > 0.1$, Gore and Crowe[14] briefly discussed the possibility of particle agglomeration in the Maeda

Correspondence concerning this article should be addressed to D. Harbottle at this current address: City College of New York, City University of New York, New York, NY 10031; e-mail: dharbottle@che.ccny.cuny.edu.

et al.[17] study leading to additional flow effects that were not observed in the other studies considered.

Several authors have considered the turbulence modulation problem looking at different variables such as particle rotation,[18] particle interference,[19] particle shape,[20] and bidisperse systems[21] confirming that the demarcation in turbulence intensity augmentation/attenuation is not so simply described by $d_p/l_e \approx 0.1$. Hadinoto et al.[22] studied the gas flow turbulence properties of 70 and 200 μm glass beads in a vertical pipe. The authors highlighted the importance of *Re* when describing turbulence modulation. For a dispersion of 70 μm glass beads, the authors observed a demarcation in the influence of particles on turbulence intensity between $13{,}800 < Re < 20{,}800$, and the 200 μm particle dispersion displayed continual enhancement in turbulence intensity with increasing *Re*. By underlining the turbulence intensity dependency on *Re*, the authors commented that such observations provide support for the work of Maeda et al.[17] and of others which do not satisfy the general demarcation rules.[14]

The work of Maeda et al.[17] and especially the comments made by Gore and Crowe[14] are of particular interest in this study. To the authors' knowledge, the effect of particle aggregates (clusters) on turbulence intensity has received little attention to date, with only Hagiwara et al.[23] considering the effect of copper particle clusters on the near wall turbulence intensity. However, the choice of heavy particles in the present work provides an additional variable (sedimentation) which is not considered in other turbulence modulation studies. Therefore, this study investigates the influence of particle aggregates on turbulence modulation when sedimentation effects are considered negligible.

Aggregate formation

Aggregates are commonly formed when solids become surface active, either by static charging in powder flow or ionization when dispersed in an aqueous solution. The mechanism of growth and the aggregate size and shape is a well-understood science.[24,25] In aqueous dispersions, very fine particles (colloids) exhibit extremely low inertial forces; as a result, their surface charge plays a significant role in their interaction and therefore the aggregate structure. The strength of interaction between neighboring colloidal particles can be suitably described by the DLVO theory[26,27] which gives the total interaction potential (V_{tot}) as the summation of the attractive van der Waals potential (V_A) and the electrical double layer repulsive potential (V_R) (Eq. 1):

$$V_{tot} = V_A + V_R = \frac{aA_H}{12H^2} + \frac{2\pi a\varepsilon_0\kappa\zeta^2 e^{\kappa H}}{1 + e^{-\kappa H}} \quad (1)$$

with a being the particle radius, A_H the effective Hamaker constant, H the surface-surface separation distance, ε the dielectric constant of the medium, ε_0 the permittivity of a vacuum, κ the inverse Debye length and ζ the zeta potential. The attractive component, which is always present, is material specific and is caused by dipolar fluctuations of the atoms, with the force of interaction decaying rapidly with surface-surface separation distance. The repulsive component arises as a result of counter-ion interaction with the charged surface. Entropy considerations mean that the counter-ion charges are not restricted to a surface adsorbed layer but are distributed within in a finite volume known as the electrical double layer, where electrical neutrality between the particle and the counter-ions is achieved. However, when two particles approach one another, overlap of the electrical double layers results in a local nonequilibrium concentration of counter-ions which is osmotically unfavorable and hence leads to repulsion.[28] The strength of the repulsive interaction is influenced by the size of the surface charge and the volume of the electrical double layer around the particle. At high electrolyte concentrations, the extension of the double layer away from the surface is reduced, thus lowering the energy barrier (kT) for interaction. Depending upon the size of the thermal energy barrier, the physical properties of the solids and the kinetic energy of the system, particles upon contact can either translate past one another or stick immediately.

In this study, the inter-particle strength is controlled by varying the ionic concentration of a monovalent electrolyte (KNO_3). An increase in the electrolyte concentration results in a decrease of the repulsive potential, thus increasing the

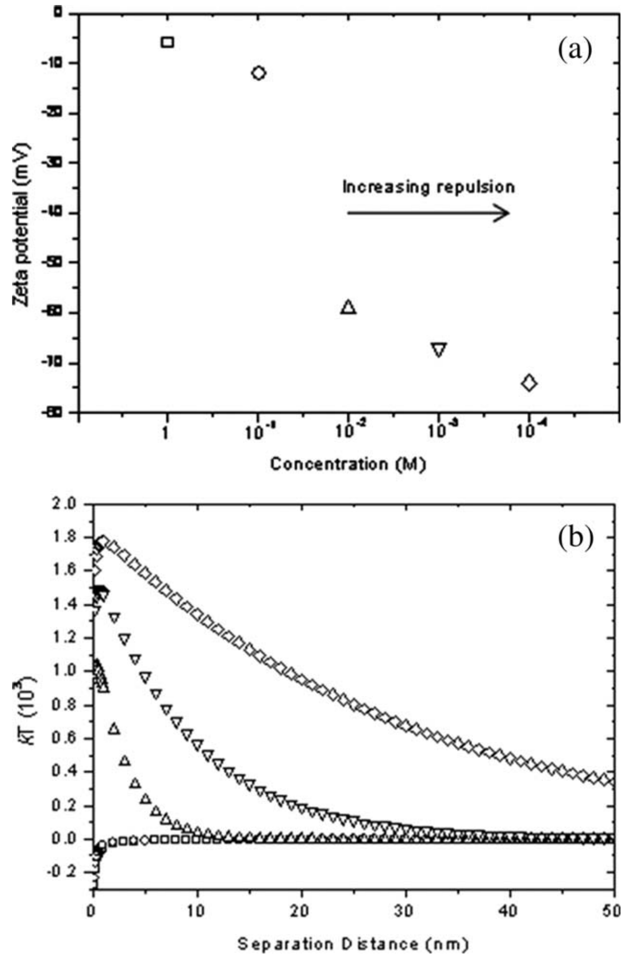

Figure 1. (a) Fuso silica zeta potential as a function of the ionic concentration (KNO_3) (pH maintained at pH6); total interaction potential determined theoretically from the DLVO relationship (Eq. 1).

Symbols correspond to those in Figure 1(a).

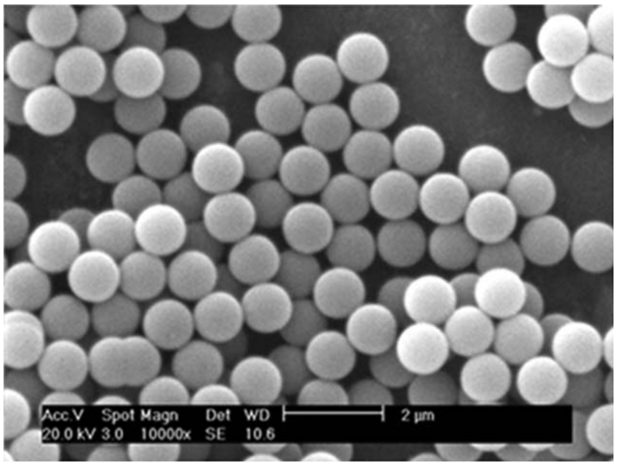

Figure 2. Fuso silica spheres SEM.

potential for interaction. Figure 1a shows the change in the zeta potential with increasing electrolyte concentration for the silica spheres used in the current study, measured using a Malvern Instruments Zetasizer Nano. Figure 1b shows the total interaction energy between two approaching spheres determined theoretically from the DLVO relationship. Zeta potentials and ionic concentrations correspond with those values presented in Figure 1a.

Materials

An ultra high purity (> 99.5% SiO_2), near mono-disperse, silica sample (SP-1B) was obtained from Fuso Chemical Co., Osaka, Japan (Figure 2). This silica sample had a density of 2.26 g/cm^3 (measured using Micromeritics AccuPyc 1330 Pycnometer), and a mean particle diameter of 0.79 μm, measured using a centrifugal sedimentation particle size analyser supplied by CPS Instruments Europe. All chemicals and other reagents were of analytical grade and were supplied by Aldrich Chemical Company (UK). The silica particles were dispersed KNO_3 electrolyte solutions (1M or 10^{-4}M), and all pH adjustments were made using complementary acid (HNO_3) and base (KOH). All water used throughout this study was Milli-Q® grade water with a conductivity ~0.05 μs/cm.

Experimental Methods

An open, re-circulating 26 mm N.B. pipe loop with PVC-U (International Plastic Systems, UK) and DURAN® glass piping (SCHOTT, UK) was constructed for the study (see Figure 3). The loop contained a 5.5 m test section of clear pipe which was secured to a horizontally levelled bench, with an outbound and inbound length of 2.3 and 2.5 m, respectively, and with the test section preceded by a disturbance free approach length which allowed the development of fully developed flow. A 620 SN/RE (Watson-Marlo w, UK) pump with a 17 mm Marprene TM tubing element provided flow rates up to Re = 11,000, with small pulsations removed using a pulsation dampener. A magnetic inductive flow meter (Krohne Optiflux, Krohne, Germany) with a 6 mm measurement bore (fused ceramic lining and platinum electrodes) capable of measuring flow rates up to Re = 15,000 was installed on a vertical section of piping.

Ultrasonic Doppler velocity profiling[29] was used to measure the turbulence properties of dispersed and aggregated colloidal silica suspensions in the pipe loop. Silica suspensions were prepared in 40 l batches to ~5.5% by volume 24 h in advance of the pipe loop study. Suspension pH was adjusted to pH6 using 5M complementary analytical grade acid and base, with the suspension periodically agitated to disperse the solids prior to being transferred to the pipe loop feed tank.

An ultrasonic probe positioned in the fully developed flow region of the pipe loop and at 45° to the flow axis submerged 1 mm into the flow stream was used to collect 512 velocity profiles over a 30-s period. Flow profiles were collected at different flow rates between 7.5 × 10^{-1} m^3/h and 5 × 10^{-2} m^3/h, with the data collected after 1 min of steady-state flow. Turbulence was determined from the root-mean square (RMS) values (u') of the streamwise component of the flow, where the RMS is given as:

$$u = \left[\frac{1}{n}\sum_{i=1}^{n}(u - U)^2\right]^{0.5} \qquad (2)$$

In the equation, u is the instantaneous velocity and U the mean streamwise velocity.

Results and Discussion

The streamwise turbulence intensity (TI = RMS/depth-averaged streamwise velocity) of a dispersed and aggregated colloidal suspension, and a particle-free flow, was measured radially from the pipe wall at regular intervals. Considering two different flow rates at Re = 5200 and Re = 7800, Figure 4 shows an enhancement in the near wall turbulence for an aggregated suspension flow (Figure 6 shows the silica aggregates formed in the high electrolyte environment). Turbulence modulation in the near wall region can be a function of the particle-fluid, particle-wall, particle-particle, and fluid-wall interactions. With the particle Reynolds numbers for the dispersed particle and aggregate calculated to be 3.5 × 10^{-7} and 6.7 × 10^{-5}, respectively, and the characteristic time of the energy containing eddies exceeding the particle relaxation time, it is expected that the fluid-wall interaction and

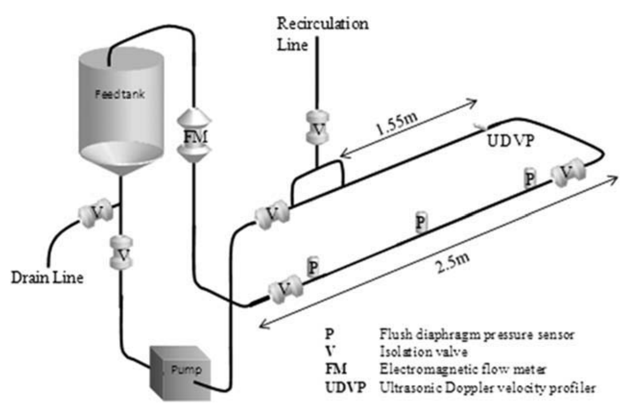

Figure 3. Schematic of the pipe loop test rig.

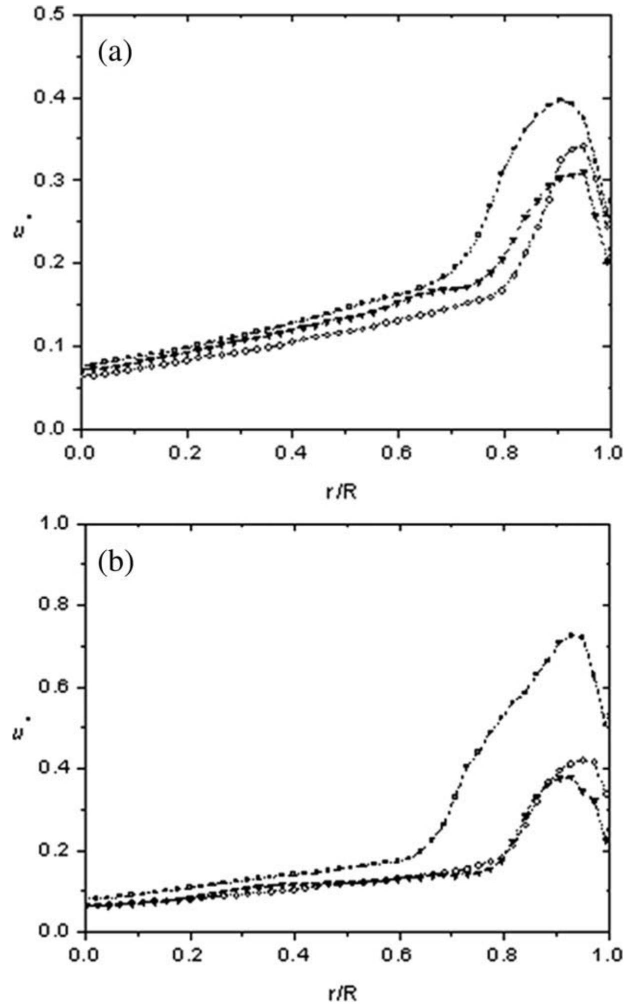

Figure 4. Streamwise turbulence intensities. Symbols: square—1M KNO_3 (5.7 vol %), circle—10^{-4}M KNO_3 (5.5 vol %), solid triangle—water. (a) *Re* = 7800 and (b) *Re* = 5200.

the particle-fluid interaction do not significantly contribute to the observed turbulence modulation. Therefore, it is reasonable to consider only the particle-wall and particle-particle interactions when describing the observed enhancement in turbulence. Particle-wall interactions modify fluid turbulence as particles "bounce" and "roll" along the pipe invert generating small scale fluctuations in the local flow field, while particle-particle interactions describe the fluctuations and disturbances in the flow field caused by colliding particles.

In this study, the experimental conditions were chosen such that the minimum transport velocities of the suspensions are exceeded. Therefore, densification of the suspension toward the pipe invert was not expected and was not observed. The observed turbulence enhancement may in part be associated with the increased particle diameter and particle mass of the aggregates, which when colliding with the pipe wall creates a larger disturbance in the flow field. Additionally, with increased size and mass, colliding aggregates would be expected to generate greater disturbances in the local flow field with respect to two colliding single colloidal particles.

Table 1. Velocity Gradients in the Near Well Region $y^+ < 30$. Units: ux mm/s, r/R(y) mm, *Re* = 7500

	du_x/dy
1M KNO_3	−75.4
10^{-4}M KNO_3	−61.7
Particle free	−66.4

It should be noted that the particle sizes considered in this study and the observed changes in turbulence do not satisfy the "classical" mechanisms for turbulence modulation.[14] There are two parameters which separate this study from much of the published literature: (i) the solids concentration and (ii) the transportation of aggregates. Much of the published literature considers turbulence modulation effects in solid-gas flows where the volume fractions are extremely low, typically less than 1%. However, the high solid loadings in this study is not thought to contribute to the modulation in the turbulence as the dispersed suspension flow shows little variation from the particle-free flow, and in actual fact can be considered within experimental error. Therefore, the formation of aggregates in the flow and their fractal, open porous structures are believed to play a major role in modifying the turbulence. Such effects are discussed further below.

In the near wall region, differences in the turbulence intensity could also be associated with small variations in the near wall velocity gradient. With the fluid shear stress proportional to the velocity gradient, an increase in the gradient provides a more favorable environment for turbulence eddy production, and therefore additional turbulence. By comparing the buffer layer velocity gradients (see Table 1) it is

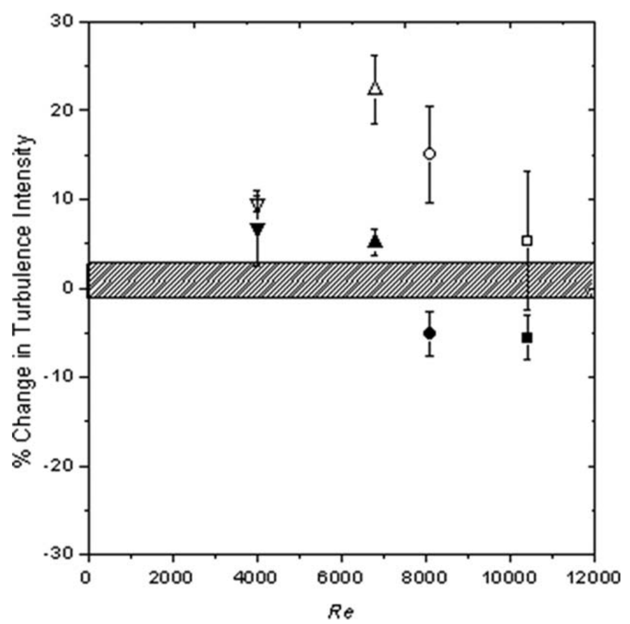

Figure 5. Percentage change in centre-line turbulence intensity relative to water: open symbols—1M KNO_3 (5.7 vol %), closed symbols—10^{-4}M KNO_3 (5.5 vol %), shaded region—water.

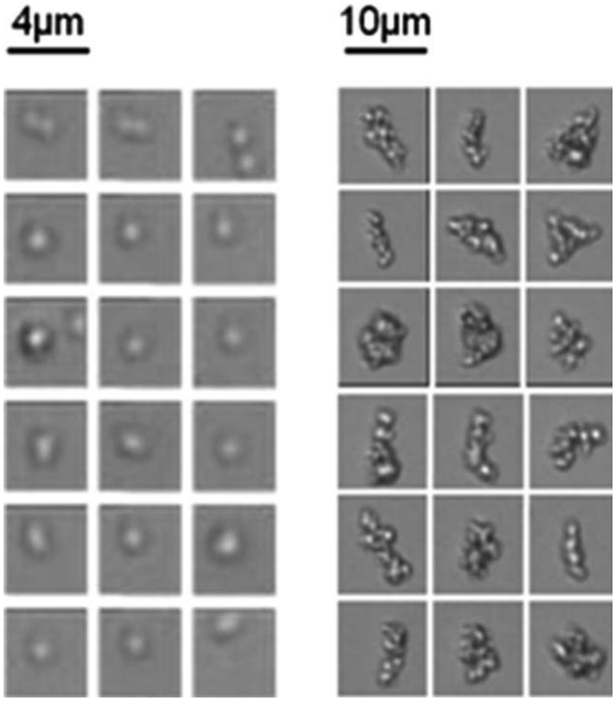

Figure 6. Colloidal particles dispersed in 10^{-4}M KNO_3 (left) and forming particle clusters in a 1M KNO_3 (right) electrolyte solution.

Images collected using Sysmex Flow Particle Image Analyser (FPIA-3000).

shown that du_x/dy 1M KNO_3 > du_x/dy 10^{-4}M KNO_3 and du_x/dy water. Therefore, the discussion on turbulence enhancement in the near wall region and the effect due to particle clusters is inconclusive due to the velocity gradient dependency. To remove such dependency, turbulence properties extending beyond the near wall region must be considered where the velocity gradient effect is sufficiently small. Figure 4 indeed shows turbulence modulation extending well beyond the near wall region (buffer layer edge: $r/R = 0.82$ ($Re = 5200$) and $r/R = 0.87$ ($Re = 7500$)), and is also observed at the pipe centerline.

Variations in the centerline turbulence intensities are summarized in Figure 5, which shows the percentage change in turbulence intensity with respect to a particle-free flow (shaded region). An average of 10 individual measurements at each velocity provided a suitable assessment of the error of uncertainty. The turbulence intensities of the dispersed suspension do not appear to deviate too much from those measured in a particle-free flow and can be considered within error. However, for the transport of an aggregated suspension there are clear differences in the turbulence properties. Away from the pipe wall, classical turbulence modulation literature would consider such changes in terms of particle-fluid and/or particle-particle interactions, i.e., vortex shedding from large particles.[14,30,31] Such effects do not appear to be the dominant factor in modifying the turbulence in the present work, with little disparity between the dispersed particle flow and the particle-free flow, suggesting that the formation of aggregates is critical to the level of turbulence modulation.

The size and shape of the dispersed particles and the particle clusters are shown in Figure 6. At high electrolyte concentrations, the particles interact forming structures which contain ~10 individual particles, either in chain-like or approximately spherical. These visible differences appear to be the dominating feature in this turbulence modulation study.

Micro-hydrodynamic disturbances at the solid-liquid interface may provide justification for the observed turbulence enhancement during the transport of particle clusters. Yang et al.[32] discussed the flow patterns through flocs (aggregates) showing that the inter-floc flows are extremely tortuous and can even reverse in flow direction. With high solid loadings, small micro-hydrodynamic disturbances can become cumulative leading to a measurable difference in the fluid turbulence. Because of the concentrated nature of the suspensions examined, which precluded the use of PIV for analysis, information on flow mapping and slip velocities could not be collected.

The effect of particle aggregates on the level of turbulence enhancement is not consistent over the flow range considered in this study (Figure 5). At low flow rates, the enhancement in turbulence intensity is measured to be around 10%, with the turbulence intensity passing through a maximum (~22% increase) before reducing to below 10% with increasing flow rate. Such behavior has been explored further and is presented in Figure 7.

The streamwise component RMS values of the particle-free flow, the dispersed, and the aggregated suspension flows are compared in Figure 7. All particle laden suspensions are

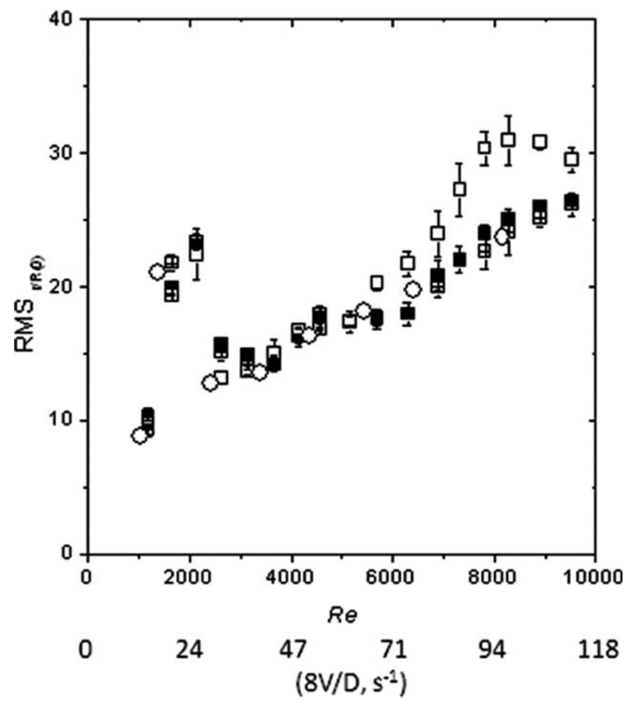

Figure 7. Root-mean square of streamwise turbulence fluctuations: solid square—10^{-4}M KNO_3 (5.5 vol %), crossed square—10^{-4}M KNO_3 (12.7 vol %), open square—1M KNO_3 (5.7 vol %), circle—water.

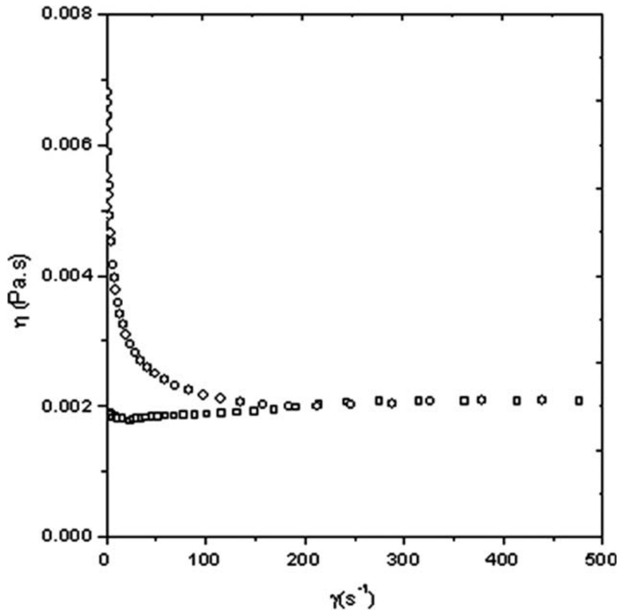

Figure 8. Flow curve, viscosity vs. shear rate: square—10^{-4}M KNO_3 (5.5 vol %), circle—1M KNO_3 (5.7 vol %).

of an equivalent solids loading (≈5.5 vol %), although a higher solids loading is also shown for the dispersed suspension. An initial peak in the RMS values for all the flows is observed around $Re = 2000$ which distinguishes the flow transition region and the presence of intermittent turbulence in the form of turbulence puffs.[33,34] Up until a critical Reynolds number is exceeded all four profiles are equal. At $Re \approx 5500$, the streamwise component RMS values for the aggregated suspension are observed to diverge and exceed those measured for the dispersed and particle-free flows. With increasing flow rate the profiles continue to diverge until a second critical Reynolds number is exceeded. At $Re \approx 8000$, the streamwise component RMS values for the aggregated suspension begin to converge with the dispersed suspension and particle-free flow profiles. The two critical Reynolds numbers are thought to be related to the onset of turbulence enhancement due to micro-hydrodynamic disturbances, and the onset of aggregate breakup, once the fluid shear stress is sufficient to overcome the normal force of particle interaction. As the concentration of aggregates in the suspension gradually reduces, the level of micro-hydrodynamic disturbances also reduces until the particles are re-dispersed, and the flow becomes representative of a dispersed suspension flow.

To probe aggregate breakup further, a standard flow curve measurement was performed on both the aggregated and dispersed suspensions using a Bohlin CVO-R rheometer, see Figure 8. The flow curve for the dispersed suspension is typical of a Newtonian fluid. Such behavior is expected with strong repulsive force acting between neighboring particles. For the aggregated system a completely different behavior is observed, with the flow curve characteristic of a non-Newtonian shear thinning fluid. With increasing shear rate, the structure within the fluid which provides a resistance to flow at low shear is gradually broken. The reduction in the suspension viscosity for the aggregated system corresponds with the breakup of aggregates.

Comparing the shear rate vs. viscosity profiles (Figure 8) and the pipeline pseudo-shear rate (8V/D) vs. RMS profiles (Figure 7), the critical shear rate at which the aggregate and the disperse suspensions exhibit similar physical properties (equal viscosities and RMS values) correspond within reasonable agreement. The maximum flow rate in the pipe flow rig limits the maximum pseudo-shear rate to 118/s, therefore, full divergence of the two profiles cannot be observed. Full divergence is measured at 170/s using the rheometer and is observed to be greater than 118/s in the pipe flow study.

Conclusions

The turbulence properties of colloidal suspensions have been shown to be sensitive to the particle-particle interaction energy. Colloidal suspensions prepared at high electrolyte concentrations are observed to form aggregates in the suspension, with the aggregates contributing to the enhancement in turbulence over a given flow range. Silica aggregates formed chain-like and spherical clusters, with the enhancement in turbulence believed to be associated with micro-hydrodynamic fluid disturbances at the solid-liquid interface. Turbulence enhancement with respect to particle-free flows is observed once a critical Reynolds number is exceeded ($Re \approx 5500$); with increasing enhancement measured until a second critical Reynolds number is exceeded ($Re \approx 8000$). Above $Re = 8000$, the fluid shear is sufficient to cause significant breakup of the aggregates in the flow leading to a reduction in the micro-hydrodynamic disturbances and therefore a reduction in turbulence production. With increasing flow rate, the turbulence properties of the aggregated suspension begin to resemble those observed for dispersed suspensions and particle-free flows. Rheological data showed that the aggregate and dispersed suspensions display similar physical properties (viscosity) at a shear rate greater than 170/s. Unfortunately, such high shear rates could not be obtained in the pipe flow loop, and as such a full correlation between the flow curve and the RMS profiles could not be made.

For colloidal/very fine particulate suspensions, ''classical'' turbulence modulation theory would indicate no effect on the turbulence; however, this study has shown a dependency on aggregate formation. To date, there has been little discussion linking turbulence modulation to the formation of particle clusters. With improving measurement technologies and an ever increasing demand to manufacture finer material, such multiphase flows systems are becoming more common in industrial processing, and as such, studies focusing on fine particle transport are of great interest.

Acknowledgments

The authors would like to thank Dr Jeffrey Peakall and Dr Gareth Keevil for providing access to the Sorby Environmental Fluid Dynamics Laboratory in the School of Earth and Environment at the University of Leeds, as well as for their continued technical support throughout the project. This work was carried out as part of the TSEC programme KNOO and as such the authors are grateful to the EPSRC for funding under grant EP/C549465/1. The authors also wish to express their gratitude to the National Nuclear Laboratory for providing further financial assistance.

Literature Cited

1. Newitt DM, Richardson JF, Shook CA. Hydraulic conveying of solids in horizontal pipes. II. Distribution of particles and dip velocities. Proceedings on the Symposium Interaction Fluids Particles London, 1962:87–100.
2. Turian RM, Yuan TF. Flow of slurries in pipelines. *AIChE J*. 1977;23:232–243.
3. Gillies RG, Shook CA. A deposition velocity correlation for water slurries. *Canad J Chem Eng*. 1991;69:1225–1227.
4. Durand R, Condolios E. The hydraulic transport of coal and solid materials in pipes. Proceedings of a Colloquium on the Hydraulic Transport of Coal, 1952:39–52.
5. Thomas DG. Transport characteristics of suspensions. VI. Minimum transport velocity for large particle size suspensions in round horizontal pipes. *AIChE J*. 1962;8:373–378.
6. Thomas AD. Predicting the deposit velocity for horizontal turbulent pipe flow of slurries. *Int J Multiphase Flow*. 1979;5:113–129.
7. Wasp EJ, Slatter PT. Deposition velocities for small particles in large pipes. 12th International Conference on the Transport and Sedimentation of Solid Particles, 2004:671–680.
8. Chapman BK, Leighton DT Jr. Dynamic viscous resuspension. *Int J Multiphase Flow*. 1991;17:469–483.
9. Leighton D, Acrivos A. Viscous resuspension. *Chem Eng Sci*. 1986;41:1377–1384.
10. Ravisangar V, Dennett KE, Sturm TW, Amirtharajah A. Effect of sediment pH on resuspension of kaolinite sediments. *J Environ Eng*. 2001;127:531–538.
11. Shauly A, Wachs A, Nir A. Shear-induced particle resuspension in settling polydisperse concentrated suspension. *Int J Multiphase Flow*. 1999;26:1–15.
12. Parthasarathy RN, Faeth GM. Turbulence modulation in homogeneous dilute particle-laden flows. *J Fluid Mech*. 1990;220:485–514.
13. Zisselmar R, Molerus O. Investigation of solid-liquid pipe flow with regard to turbulence modification. *Chem Eng J*. 1979;18:233–239.
14. Gore RA, Crowe CT. Effect of particle size on modulating turbulent intensity. *Int J Multiphase Flow*. 1989;15:279–285.
15. Best JL, Bennett S, Bridge J, Leeder M. Turbulence modulation and particle velocities over flat sands at low transport rates. *J Hydraulic Eng*. 1997;123:1118–1129.
16. Hetsroni G. Particles-turbulence interaction. *Int J Multiphase Flow*. 1989;15:735–746.
17. Maeda M, Hishida K, Furtani T. Velocity distributions of air-solid suspension in upward pipe flow (effect of particles on air velocity distribution). *Trans Jpn Soc Mech Eng Ser B*. 1980;46: 2313–2320.
18. Best JL. The influence of particle rotation on wake stability at particle Reynolds numbers, $Re_p < 300$—Implications for turbulence modulation in two-phase flows. *Int J Multiphase Flow*. 1998;24: 693–720.
19. Tsuji Y, Morikawa Y. LDV measurements of an air-solid two phase flow in a horizontal pipe. *J Fluid Mech*. 1982;120:385–409.
20. Ljus C, Johansson B, Almstedt AE. Turbulence modification by particles in a horizontal pipe flow. *Int J Multiphase Flow*. 2002;28: 1075–1090.
21. Yarin LP, Hetsroni G. Turbulence intensity in dilute two-phase flows—1. Effect of particle size distribution on the turbulence of the carrier fluid. *Int J Multiphase Flow*. 1994;20:1–15.
22. Hadinoto K, Jones EN, Yurteri C, Curtis JS. Reynolds number dependence of gas-phase turbulence in gas-particle flows. *Int J Multiphase Flow*. 2005;31:416–434.
23. Hagiwara Y, Murata T, Tanaka M, Fukawa T. Turbulence modification by the clusters of settling particles in turbulent water flow in a horizontal duct. *Powder Technol*. 2002;125:158–167.
24. Lindsay HM, Lin MY, Weitz DA, Sheng P, Chen Z, Klein R, Meakin P. Properties of fractal colloid aggregates. *Faraday Discuss Chem Soc*. 1987;83:153–165.
25. Asnaghi D, Carpineti M, Giglio M, Sozzi M. Coagulation kinetics and aggregate morphology in the intermediate regimes between diffusion-limited and reaction-limited cluster aggregation. *Am Phys Soc Phys Rev A*. 1992;45:1018–1023.
26. Derjaguin BV, Landau L. Theory of the stability of strongly charged lyophobic sols and of the adhesion of strongly charged particles in solutions of electrolytes. *Acta Physicochem URSS*. 1941;14:633–662.
27. Verwey EJW, Overbeek JTG. *Theory of the Stability of Lyophobic Colloids*. Amsterdam: Elsevier, 1948.
28. Biggs S. Aggregate structures and solid-liquid separation processes. *Kona*. 2006;24:41–53.
29. Takeda Y. Velocity profile measurement by ultrasound Doppler shift method. *Int J Heat Fluid Flow*. 1986;7:313–318.
30. Achenbach E. Vortex shedding from spheres. *J Fluid Mech*. 1974;62:209–221.
31. Kim S, Lee KB, Lee CG. Theoretical approach on the turbulence intensity of the carrier fluid in dilute two-phase flows. *Int J Heat Fluid Flow*. 2005;32:435–444.
32. Yang Z, Peng XF, Lee DJ, Ay S. Advective flow in spherical floc. *J Colloid Interface Sci*. 2007;308:451–459.
33. Wygnanski IJ, Champagne FH. On transition in a pipe. Part 1. The origin of puffs and slugs and the flow in a turbulent slug. *J Fluid Mech*. 1973;59:281–335.
34. Wygnanski I, Sokolov M, Freidman D. On transition in a pipe. Part 2. The equilibrium puff. *J Fluid Mech*. 1974;69:283–308.

Manuscript received Oct. 27, 2009, revision received Apr. 5, 2010, and final revision received July 22, 2010.